RESEARCH ARTICLE

Correspondence to:
L. E. Simms,
simmsl@augsburg.edu

Analysis of the effectiveness of ground-based VLF wave observations for predicting or nowcasting relativistic electron flux at geostationary orbit

Laura E. Simms[1], Mark J. Engebretson[1], A. J. Smith[2], Mark Clilverd[3], Viacheslav Pilipenko[4], and Geoffrey D. Reeves[5]

[1]Augsburg College, Minneapolis, Minnesota, USA, [2]VLF ELF Radio Research Institute, Bradwell, UK, [3]British Antarctic Survey, Cambridge, UK, [4]Institute of the Physics of the Earth, Moscow, Russia, [5]Los Alamos National Laboratory, Los Alamos, New Mexico, USA

Abstract Poststorm relativistic electron flux enhancement at geosynchronous orbit has shown correlation with very low frequency (VLF) waves measured by satellite in situ. However, our previous study found little correlation between electron flux and VLF measured by a ground-based instrument at Halley, Antarctica. Here we explore several possible explanations for this low correlation. Using 220 storms (1992–2002), our previous work developed a predictive model of the poststorm flux at geosynchronous orbit based on explanatory variables measured a day or two before the flux increase. In a nowcast model, we use averages of variables from the time period when flux is rising during the recovery phase of geomagnetic storms and limit the VLF (1.0 kHz) measure to the dawn period at Halley (09:00–12:00 UT). This improves the simple correlation of VLF wave intensity with flux, although the VLF effect in an overall multiple regression is still much less than that of other factors. When analyses are performed separately for season and interplanetary magnetic field (IMF) B_z orientation, VLF outweighs the influence of other factors only during winter months when IMF B_z is in an average northward orientation.

1. Introduction

A number of studies have found an association between relativistic electron enhancement and very low frequency (VLF) magnetospheric waves measured on the ground [*Meredith et al.*, 2003; *Smith et al.*, 2004] and by satellite [*O'Brien et al.*, 2003; *Miyoshi et al.*, 2013]. As well, there are many examples of satellite observations of VLF waves leading directly to relativistic electron flux enhancement [*Horne et al.*, 2005; *Thorne et al.*, 2013; *Li et al.*, 2014; *Su et al.*, 2014; *Turner et al.*, 2014; *Xiao et al.*, 2014]. Successful models of the acceleration of seed electrons to relativistic energies by VLF waves alone have also been produced [e.g., *Albert et al.*, 2009; *Tu et al.*, 2014], as well as physics-based models incorporating wave-particle interactions as one of many key processes [*Horne et al.*, 2013].

Numerous studies have shown correlations between relativistic electron flux levels and parameters such as solar wind velocity and number density [*Blake et al.*, 1997; *Baker et al.*, 1998; *O'Brien et al.*, 2001; *Reeves et al.*, 2003, 2011; *Weigel et al.*, 2003; *Ukhorskiy et al.*, 2004; *Lyons et al.*, 2005; *Lyatsky and Khazanov*, 2008a, 2008b; *Balikhin et al.*, 2011; *Kellerman and Shprits*, 2012; *Potapov et al.*, 2012, 2014]; *Dst*, *Kp*, and *AE* indices [*Baker et al.*, 1990; *Dmitriev and Chao*, 2003; *Meredith et al.*, 2003; *Li et al.*, 2009; *Lyatsky and Khazanov*, 2008b; *Ukhorskiy et al.*, 2004]; interplanetary magnetic field (IMF) B_z [*Blake et al.*, 1997; *Iles et al.*, 2002; *Miyoshi and Kataoka*, 2008; *Miyoshi et al.*, 2013]; and ULF (ultralow frequency) wave power [*Rostoker et al.*, 1998; *Mathie and Mann*, 2000; *O'Brien et al.*, 2003; *Kozyreva et al.*, 2007; *Romanova and Pilipenko*, 2008; *Borovsky and Denton*, 2014; *Potapov et al.*, 2014]. Although a correlation between a factor and relativistic flux does not prove that factor causes increased flux, a lack of positive correlation would suggest that it is not involved in electron acceleration. However, no matter what the mechanism is, a strong correlation between a parameter and increasing relativistic flux means that factor can be used as a predictor of increased flux.

In a previous paper, we found that many solar wind and magnetosphere parameters, as well as a ULF wave index, could be used to predict relativistic electron flux levels at geostationary orbit following storms using a data-based model produced by multiple regression [*Simms et al.*, 2014]. As many of these factors are correlated among themselves, we developed models that attempted to determine which of these factors

correlated with and predicted flux best when all factors were present in the model. This extended the work of previous multifactor, data-based models [*Lyatsky and Khazanov*, 2008b; *Ukhorskiy et al.*, 2004; *Balikhin et al.*, 2011; *Kellerman and Shprits*, 2012; *Borovsky and Denton*, 2014].

However, in our previous models [*Simms et al.*, 2014], ground-based measurements of VLF magnetospheric waves (~1 kHz) showed little ability to predict enhanced relativistic electron flux 24 h later. In the present study, we suggest several possible explanations for why ground-based VLF does not work well as a predictor.

Previously, we attempted to predict flux more than 72 h after the minimum *Dst* of a storm using variables averaged over three time periods: prestorm, main phase, and early recovery phase (48 h immediately following the minimum *Dst*). ULF wave power, seed electron flux, solar wind velocity and its variation, and after-storm IMF B_z were the most significant explanatory variables in these regression models. However, any factor that operated at a short time scale on flux would be missed by this approach, as predictors were measured no less than 24 h in advance of the flux measurement. A nowcast model would be more appropriate for studying short-term actions.

Our previous paper used a daily average of VLF wave power from the Halley VLF/ELF Logger eXperiment (VELOX) instrument, which does not discriminate between chorus and hiss in several band-pass spectral windows [*Smith et al.*, 2010]. However, VLF waves may be responsible for both increases in flux due to acceleration of electrons by chorus waves and decreases due to precipitation caused by hiss [*Kessel*, 2012]. Therefore, averaging the entire 24 h magnetic local time (MLT) period may result in a measure that cannot distinguish between the opposing effects of acceleration and precipitation. In our current study, we compare the 24 h average with VLF averaged only over the dawn period (09:00–12:00 UT at Halley) when dawn chorus dominates (06:00–09:00 MLT) [*Smith et al.*, 2010].

Seasonal effects may be a third explanation for why VLF waves showed so little influence in our previous predictive models. This may be due to two reasons. First, the ground VLF wave power measured at Halley that we use may vary between seasons. Solar illumination of the ionosphere in the southern hemisphere summer months (October–February) at Halley has been found to reduce the VLF wave amplitude in the 1–3 kHz range [*Smith et al.*, 2010]. Thus, the apparent influence of VLF waves may be artificially lowered during these time periods when its measured amplitude is reduced.

Besides this measurement effect of season, the geoeffectiveness of solar wind parameters may vary by season as a result of IMF B_z orientation relative to the Earth's magnetosphere, changing as the year progresses [*Russell and McPherron*, 1973; *McPherron et al.*, 2009]. Although our previous paper controlled for a B_z effect, we did not control for season nor study how the B_z effect (or that of other parameters) might behave in different seasons.

The thrust of this current paper is therefore threefold: (1) to produce nowcast models as a complement to our predictor models to determine whether ground VLF power has more correlation with flux at more immediate time scales, (2) to study whether limiting the ground VLF measure to the dawn period results in more correlation with flux, and (3) to explore the effect of season on the ground VLF-flux correlation. The refinement of the model using these approaches may allow the use of ground VLF to predict relativistic electron flux.

To do this, we again use the technique of multiple regression. This allows the straightforward addition of predictor variables, as well as determining which predictors are most significant when all other factors are held constant [*Neter et al.*, 1985; *Simms et al.*, 2010; *Golden et al.*, 2012].

2. Methods

As described more fully in *Simms et al.* [2014], we identified 220 storms (1992–2002) with at least 72 storm-free hours after the end of recovery (when *Dst* returns above −30 nT). We used the 1.0 kHz VELOX channel of Halley VLF (this channel includes frequencies from 0.5 to 1.5 kHz) as it showed the most influence in simple correlations and the multiple regressions. This channel corresponds to an L_{max} of 7.52 and will detect VLF from *L* shells below 7.52, including those at geosynchronous orbit (*L* = 6.6) [*Smith et al.*, 2004; *Smith*, 1995]. Our initial analyses used the 24 h (MLT) average of VLF wave power. However, in later analyses, we use the average of VLF wave power only from the dawn period at Halley (09:00–12:00 UT; 06:00–09:00 MLT). This time period was chosen as that in which dawn chorus would be the strongest influence [*Smith et al.*, 2010]. Only 191 storms remained in this data set, as not all had VLF observations in this time period.
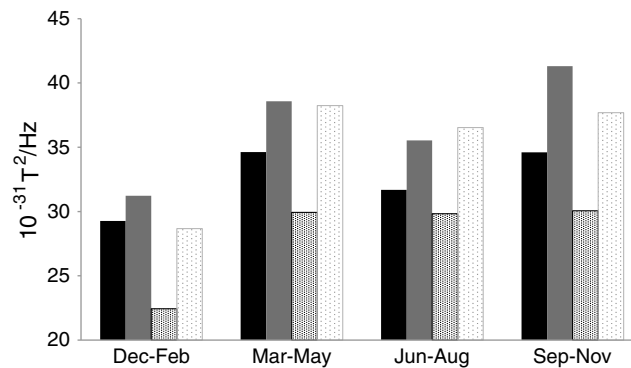
Figure 1. Ground VLF power following storms averaged by season. The black bars are the VLF averaged over 0–48 h following the minimum *Dst*. The gray bars are the VLF averaged over the late recovery (48–72 h following the minimum *Dst*). The solid bars are the VLF averaged over all hours of the day. The patterned bars are the VLF averaged over the dawn period (09:00–12:00 UT).

We obtained hourly averaged electron fluxes for relativistic electrons (>1.5 MeV) and seed electrons (75–105 keV) from several spacecraft (Los Alamos National Laboratory (LANL) geosynchronous energetic particle instruments at approximately 6.6 R_E). We calculated the maximum relativistic electron flux of these hourly averages in the 48–120 h following each storm.

As additional predictor variables, we used a ground-based ULF index [*Kozyreva et al.*, 2007] (2–7 mHz, covering local times 05:00–15:00, characterizing the maximal hourly value of ULF wave power over the entire globe). All wave power variables were $\log_{10}$ values. In addition, we obtained IMF B_z (GSM coordinates) and solar wind velocity (V_x in GSM coordinates). In preliminary analyses, we discovered that the correlation between V_x and number density was too high to allow the use of both in our multiple regression models. As number density entered the models as a negative factor, we chose to use V_x.

All variables were converted to rankit normal scores [*Sokal and Rohlf*, 1995] by assigning a rank to each observation and then replacing that rank with the value of the same ranked order statistic from a normal distribution. This transformation converted the data into a normal distribution and allowed the use of linear regression, even if the original variables were related in a nonlinear way. Statistical analyses were performed in Statistical analyses were performed in SPSS (Statistical Package for the Social Sciences) and IDL (Interactive Data Language).

We found the average of each solar wind and IMF predictive variable during two storm periods: early recovery phase (0–48 h after the minimum *Dst*) and late recovery phase (48–72 h after the minimum *Dst*). Regressions using the first time period were used to predict flux 48–120 h after the minimum *Dst*. Regressions using the second time period were used to nowcast flux. Although we included up to 120 h after the minimum *Dst* in which to find the maximum flux, most of the rise in flux occurs by 72 h and the levels remain fairly constant in the latter half of this time period [*Borovsky and Denton*, 2009]. Other variables, however, drop off during this time period, so an average of them over this entire time period would give artificially low values.

Full regression models are given for the full data set (all seasons combined), but when the data set is split into seasons, the sample sizes become too low to keep all variables in the models. The seasonal models were therefore reduced using backward elimination. This is a type of stepwise regression used to choose the most explanatory variables. This method adds all variables to the model at the beginning, then drops those which show no significant effect [*Hocking*, 1976]. After each variable is removed, a regression is run again with the reduced set, and the next variable that does not meet the criterion for inclusion dropped. The algorithm stops when all remaining predictor variables meet the significance criterion. We set the level at which to remove a variable at a *P* value >0.10. The *P* value is the estimated probability of mistakenly rejecting a null hypothesis when that hypothesis is actually true. Statistical significance is often set at $P < 0.05$, so the 0.10 criterion will conservatively include more variables in a model rather than discarding them. This method is a means of producing a model that is not overfitted while retaining all variables that may show an influence. (Other regression techniques such as ridge regression, principal component regression, or partial least squares regression (discussed in *Hastie et al.* [2009]) might be used with data sets such as this to reduce multicollinearity, but these methods either make statistical tests impossible or obscure the relative influence of predictors. For these reasons, we have continued to use ordinary least squares regression.)

In a previous study, validation of similar models (based on the same data set) was performed with a training set of a semirandom sample of four fifths of the storms (spread over all years and seasons) and the remaining one fifth as the validation set (with a similar spread over years and seasons) [*Simms et al.*, 2014].
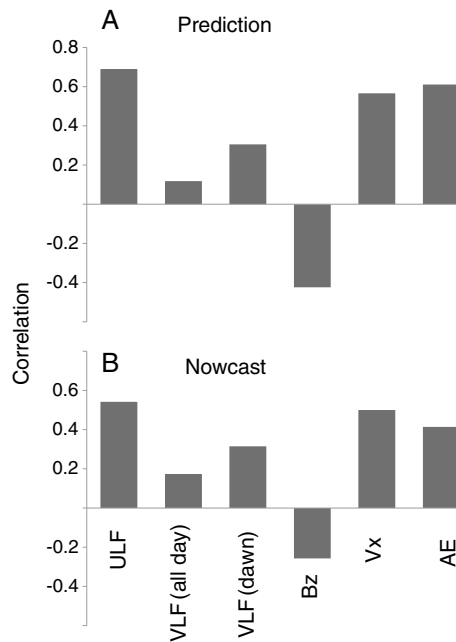
Figure 2. Correlations of variables with relativistic electron flux. All variables are averages from after the minimum Dst. (a) Predictor variables (0–48 h after the minimum Dst) and (b) nowcast variables (48–72 h after the minimum Dst). "All day" VLF averaged over all 24 h of the day and "dawn" VLF averaged over 09:00–12:00 UT.

Only 191 storms remained in the data set when VLF was averaged only over the dawn period (09:00–12:00 UT). Within this set, there were 44 storms in the December–February period, 60 in March–May, 41 in June–August, and 46 in September–November.

When models were split by IMF B_z orientation, the northward B_z category included all those storms, where the B_z averaged over the time period in question was positive (0–48 h after the minimum Dst for the prediction models and 48–72 h for the nowcast models). The southward category included those where the B_z average was negative.

3. Results

Halley ground VLF wave amplitude following storms is significantly lower during the height of southern hemisphere summer (December–February) (Figure 1). This is true of VLF waves measured in the early recovery (0–48 h after the minimum Dst—the "predictor" variable set) and in the late recovery (48–72 h after the minimum Dst—the "nowcast" variable set). It is also seen in both VLF averaged over the entire 24 h period and that averaged only during the dawn (09:00–12:00 UT) when the dawn chorus is strongest.

Of all the predictor variables, VLF averaged over the full 24 h MLT period showed the least correlation with relativistic electron flux in both the prediction and the nowcast models (Figure 2). When averaged only over 09:00–12:00 UT (dawn), VLF was somewhat more correlated with flux. We use this subset of dawn-averaged VLF power in all the remaining analyses.

Of the four VELOX frequency channels studied (0.5, 1.0, 2.0, and 4.25 kHz), the highest correlation of dawn VLF wave power (09:00–12:00 UT) with relativistic electron flux occurs with the nowcast 1.0 kHz channel (Table 1). The slightly lower correlations seen with VLF 24 h previously may suggest that VLF acts at a more immediate time scale. All other variables show modestly more correlation as predictors than as nowcasters (Figure 2).

When VLF-flux correlations are broken down by both season and IMF B_z orientation, VLF shows the highest correlation during periods of northward B_z (Figure 3). This is most pronounced in the winter months (June–August).

The full multiple regressions over all seasons show few differences between the prediction and nowcast models. Main phase seed electron flux, ULF power, V_x, and IMF B_z are significant, correlates when measured in the early recovery (0–48 h following the minimum Dst; prediction—Figure 4a) and when measured in the late recovery (48–72 h following the minimum Dst; nowcast—Figure 4b). VLF power is not a significant influence in either the prediction or the nowcast model when all seasons are combined.

As nowcast and prediction models were similar, and as nowcast simple correlations were slightly higher, only
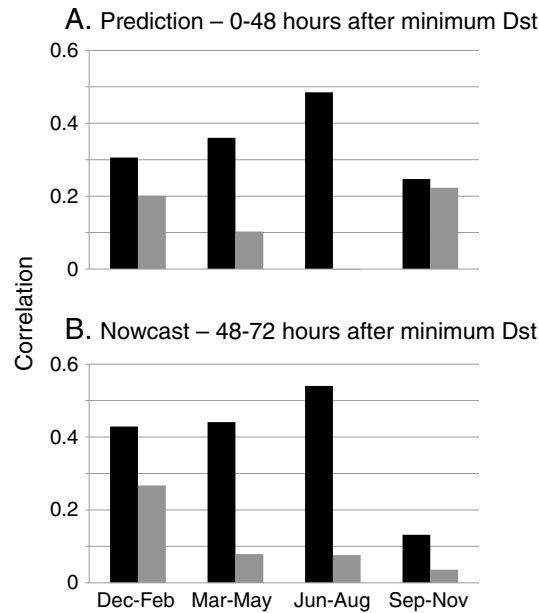
Table 1. Correlation of VLF Wave Power (09:00–12:00 UT) With Relativistic Electron Flux (Rankit Transformations)[a]

VLF Channel	Prediction[b]	Nowcast[c]	L_{max}
0.5 kHz	0.238[d]	0.254[d]	9.47
1.0 kHz	0.308[d]	0.316[d]	7.52
2.0 kHz	0.054	0.038	5.96
4.25 kHz	−0.043	−0.025	4.64

[a]L_{max} from *Smith et al.* [2004]. N = 190 storms.
[b]VLF measured 0–48 h after the minimum Dst.
[c]VLF measured 48–72 h after the minimum Dst.
[d]Significant correlation ($P < 0.05$).

Figure 3. VLF-flux correlations by season and IMF B_z orientation. (a) Prediction model (predictors measured 0–48 h after the minimum Dst) and (b) nowcast (predictors measured 48–72 h after the minimum Dst). The black bars are the northward IMF B_z, and the gray bars are the southward IMF B_z. IMF B_z orientation is northward if average B_z 0–48 h after the minimum Dst was positive and southward if the average B_z was negative. Correlation of 0.002 of VLF with relativistic electron flux during June–August southward B_z is too small to appear on this graph.

the nowcast data are used in the seasonal breakdown analyses. When seasons are analyzed separately, the sample sizes became too low to keep all variables in the models. Therefore, reduced models were produced by backward elimination stepwise regression, in which most nonsignificant variables ($P > 0.10$) were dropped. Figure 5 shows nowcast models by season (explanatory variables averaged over the late recovery—48–72 h after the minimum Dst). VLF wave power is retained only in the June–August period, although it is not statistically significant.

As the VLF influence appears to vary by both season and IMF B_z orientation, we analyzed subsets broken down by both these factors (Figure 6). We show only those regression models in which VLF showed a significant influence (March–May and June–August, the winter months in the southern hemisphere). VLF was the only significant factor during periods of northward B_z in these winter months, but it was not a factor during periods of southward B_z in winter months.

4. Discussion

As in our previous study [*Simms et al.*, 2014], other variables (seed electron flux, ULF wave index, V_x, and IMF B_z) show more ability to predict relativistic electron flux than VLF waves, whether in simple correlation analysis or in multiple regression models. However, VLF wave power was found to correlate with relativistic electron flux in other studies of both ground and satellite VLF [*Meredith et al.*, 2003; *O'Brien et al.*, 2003; *Smith et al.*, 2004; *Lyons et al.*, 2005; *Miyoshi et al.*, 2013; *Thorne et al.*, 2013]. We hypothesize several reasons why we may be finding different results.

Within the broad class of VLF waves, chorus waves are thought to accelerate electrons, while hiss is believed to cause electron precipitation [*Kessel*, 2012]. Both dawn chorus and afternoon hiss are picked up by the Halley VELOX instruments [*Smith et al.*, 2010]. Averaging the two together may result in a measure that cannot
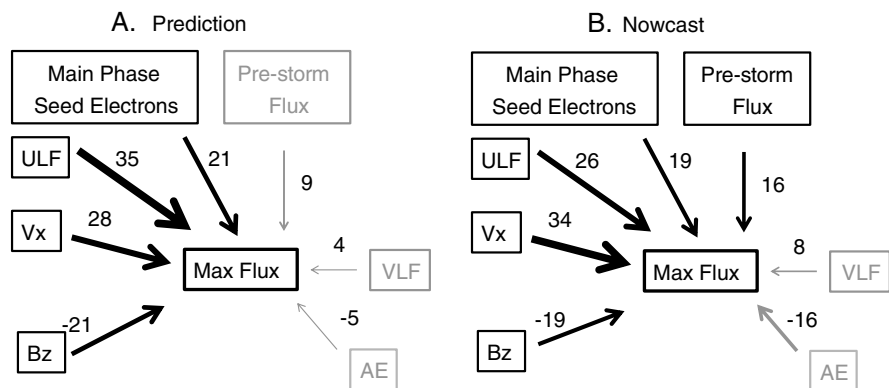

Figure 4. Influence of parameters over all seasons in (a) the prediction model and (b) the nowcast model. The numbers are the standardized regression coefficients × 100. The black arrows represent significant parameters ($P < 0.05$); the gray arrows represent nonsignificant variables.
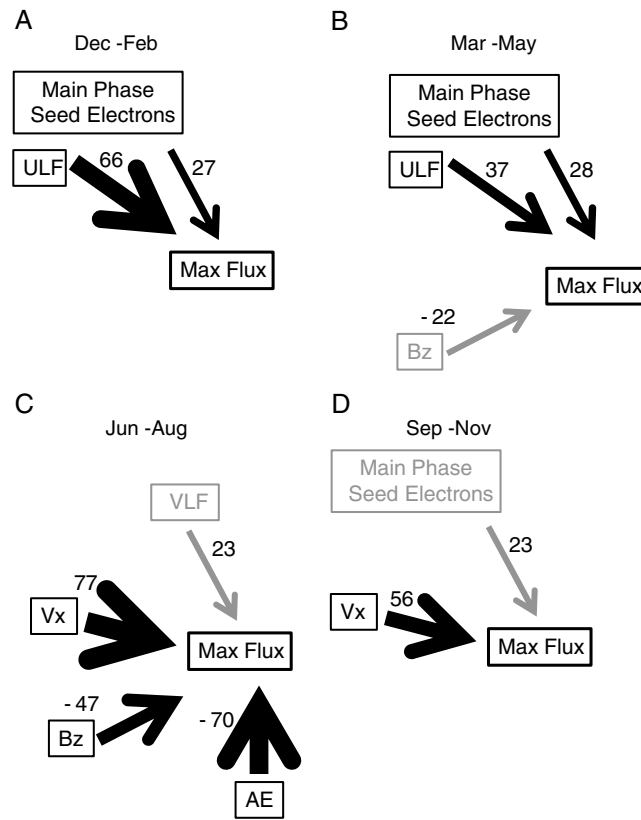
Figure 5. Nowcast model: influence of parameters by season (reduced models). Explanatory variables averaged over 48–72 h following the minimum Dst. (a) December–February ($n = 44$), (b) March–May ($n = 60$), (c) June–August ($n = 41$), and (d) September–November ($n = 46$). The numbers are the standardized regression coefficients × 100. The black arrows represent significant parameters ($P < 0.05$); the gray arrows represent nonsignificant variables.
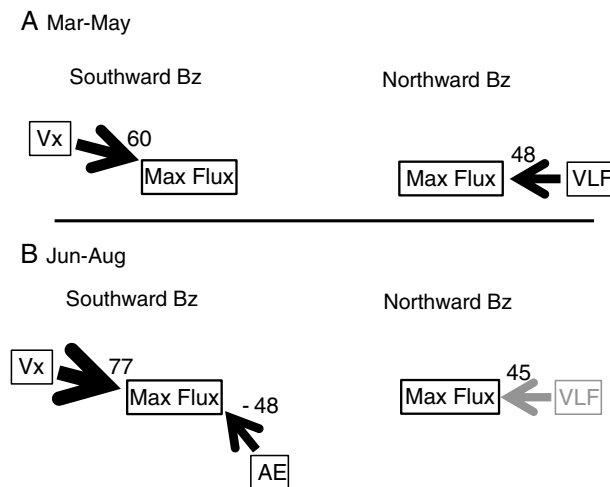

Figure 6. Reduced nowcast models for southern hemisphere winter months broken down by IMF B_z orientation. (a) March–May (southward $n = 32$ and northward $n = 28$) and (b) June–August (southward $n = 24$ and northward $n = 17$). IMF B_z orientation is northward if B_z averaged over the 48–72 h following the minimum Dst was positive and southward if the average B_z was negative.

distinguish between the opposing effects of acceleration and precipitation. Halley VELOX (at L shell 4.5) is located such that it is close to the quiet time plasmapause field line footprint. Thus, at ~1 kHz, it will see a combination of VLF chorus waves (occurring outside the plasmapause) and plasmaspheric hiss (occurring inside the plasmapause), depending on the local time. This could reduce the correlation with poststorm relativistic fluxes, as plasmaspheric hiss takes no part in the electron acceleration process and may even be responsible for electron loss. By limiting our observations to the 09:00–12:00 UT period (dawn at Halley), we hoped to boost the contribution of dawn chorus which is hypothesized to cause electron acceleration. Limiting observations to the dawn period did improve the simple correlation we found between VLF wave power and relativistic flux enhancements, thus confirming the VLF correlation found in other studies that followed VLF waves [*Meredith et al.*, 2003; *O'Brien et al.*, 2003; *Smith et al.*, 2004; *Lyons et al.*, 2005; *Miyoshi et al.*, 2013]. However, the magnitude of the correlation between flux and VLF wave power is still lower than that of most of the other tested variables.

Second, VLF waves may act more immediately. In our previous paper, we used average parameter values from the first 48 h following the minimum Dst to predict the rise in flux more than 48 h after the minimum Dst. However, a parameter that acted to increase flux within minutes or hours might have been missed with this approach. In our current study, we explore this possibility by comparing correlations and regression models between a prediction model (independent variables averaged over the first 48 h) versus a nowcast model (independent variables averaged over the late recovery, 48–72 h after the minimum Dst). However, the nowcast correlation of 1.0 kHz VLF power is only slightly higher (Table 1). While this may account for some of the low correlation, it is not a major factor.

Although the simple correlation of VLF wave power with relativistic electron flux can be increased by restricting the VLF measurement to the dawn period (09:00–12:00 UT) and, to a lesser extent, by using a nowcast model, VLF still loses all significant influence in multiple regressions when other predictors are included in the model. This may be due to several other processes.

First, ground-measured VLF power may only be a significant explanatory factor in certain seasons. Ground VLF amplitude is reduced during summer months due to solar illumination of the ionosphere. Previously, this effect was found to reduce VLF amplitude in the 1–3 kHz range in the southern hemisphere summer months (October–February) at Halley, Antarctica [*Smith et al.*, 2010]. We also found lower VLF amplitude in the December–February (summer) period as compared to other quarters of the year (Figure 1). As might be expected, our highest correlations with flux were in the winter months (March–May and June–August) but only when average recovery IMF B_z was in the northward direction.

The effectiveness of VLF waves only when IMF B_z is oriented northward would seem to contradict what is found in other studies. *Miyoshi et al.* [2013] found that relativistic electron enhancements were more likely during southward B_z orientation, during which time VLF whistler waves also showed greater power. They concluded from this that the VLF acceleration of electrons was not effective during northward B_z, when both flux and VLF power were low. However, our correlation and regression analyses do not support this hypothesis. The only regression models in which VLF was found to be a significant factor were those from the winter months (March–May and, to a lesser extent, June–August) when only storms with average northward B_z were considered. Possibly, the reduction in other factors may mean that they are less effective, allowing the VLF effect to be seen, or it may be that during periods of northward B_z, the Halley VELOX instrument is getting a truer picture of VLF power at geosynchronous orbit where the acceleration is taking place.

The field of view of the Halley VELOX receiver will be strongly influenced by the levels of subionospheric attenuation associated with propagation of the waves from more distant field lines, such as those of geosynchronous orbit at $L = 6.6$. The subionospheric distance of at least ~700 km from the $L = 6.6$ field line ionospheric exit point to the Halley receiver is equivalent to ~20 dB attenuation at 1 kHz during the daytime (or summer) compared with ~10 dB during the winter [*Challinor*, 1967]. Thus, the receiver field of view is significantly wider during the winter months (June–August) than at other times. The slightly higher correlation between VLF waves and relativistic electron flux during June–August occurs when the VELOX field of view is able to pick up VLF wave power from the widest range of L shells.

Additionally, ground VLF observations are thought to be exclusively ducted waves, while satellite observations are rarely, if ever, made inside ducts [*Walker*, 1971; *Burgess and Inan*, 1993]. The relationship between the two depends strongly on the efficiency of wave coupling into and out of ducts, which is probably quite variable [*Rodger et al.*, 2010]. Electron acceleration can involve both ducted and nonducted chorus, but at a given moment in time, satellite observations in the nonducted region may rarely correlate with ground observations along the ducts. Thus, it is not surprising that the Halley ground-based VLF wave power shows only a modest correlation (0.315 at best) with relativistic electron flux, while satellite VLF observations show more association.

5. Conclusion

Our previous paper [*Simms et al.*, 2014] found little correlation between ground VLF wave power and relativistic flux enhancement, although several previous studies had shown such a correlation. We have explored several possible explanations. We hypothesized that the VLF effect may be more immediate than that of the other explanatory variables, occurring within minutes or hours of the flux enhancement. However, a nowcast correlation of the VLF-flux correlation is only slightly higher when VLF waves are measured in the late recovery (48–72 h after the minimum *Dst*) than when they are measured immediately after the minimum *Dst*. Thus, the VLF waves do not appear to act more immediately than other factors.

Limiting the ground VLF observations to 09:00–12:00 UT, the dawn period at Halley, when chorus is at a maximum, had more impact on the correlation between VLF and relativistic electron flux. However, a multiple regression model using this refined measure still resulted in VLF having little influence when other factors are present.

The simple correlation of ground VLF with flux is somewhat higher during winter months (June–August in the southern hemisphere) and much higher when only storms with average northward IMF B_z during recovery are

considered. Multiple regressions during these time periods show ground VLF to be a major correlate of relativistic electron flux, even when other factors are allowed in to the model.

However, ground VLF is not a useful parameter for predicting relativistic electron flux during most of the year. Satellite VLF measurements may be more strongly correlated with flux than ground-measured VLF. In the future, we plan to compare the correlations of ground and satellite VLF waves with relativistic electron flux and to determine if satellite VLF measurements may be more useful in producing a predictive model.

References

Albert, J. M., N. P. Meredith, and R. B. Horne (2009), Three-dimensional diffusion simulation of outer radiation belt electrons during the 9 October 1990 magnetic storm, *J. Geophys. Res.*, *114*, A09214, doi:10.1029/2009JA014336.

Baker, D. N., R. L. McPherron, T. E. Cayton, and R. W. Klebesadel (1990), Linear prediction filter analysis of relativistic electron properties at 6.6 R_E, *J. Geophys. Res.*, *95*, 15,133–15,140, doi:10.1029/JA095iA09p15133.

Baker, D. N., X. Li, J. B. Blake, and S. Kanekal (1998), Strong electron acceleration in the Earth's magnetosphere, *Adv. Space Res.*, *21*(4), 609–613.

Balikhin, M. A., R. J. Boynton, S. N. Walker, J. E. Borovsky, S. A. Billings, and H. L. Wei (2011), Using the NARMAX approach to model the evolution of energetic electrons fluxes at geostationary orbit, *Geophys. Res. Lett.*, *38*, L18105, doi:10.1029/2011GL048980.

Blake, J. B., D. N. Baker, N. Turner, K. W. Ogilvie, and R. P. Lepping (1997), Correlation of changes in the outer-zone relativistic-electron population with upstream solar wind and magnetic field measurements, *Geophys. Res. Lett.*, *24*, 927–929, doi:10.1029/97GL00859.

Borovsky, J. E., and M. H. Denton (2009), Relativistic-electron dropouts and recovery: A superposed epoch study of the magnetosphere and the solar wind, *J. Geophys. Res.*, *114*, A02201, doi:10.1029/2008JA013128.

Borovsky, J. E., and M. H. Denton (2014), Exploring the cross correlations and autocorrelations of the ULF indices and incorporating the ULF indices into the systems science of the solar wind-driven magnetosphere, *J. Geophys. Res. Space Physics*, *119*, 4307–4334, doi:10.1002/2014JA019876.

Burgess, W. C., and U. S. Inan (1993), The role of ducted whistlers in the precipitation loss and equilibrium flux of radiation belt electrons, *J. Geophys. Res.*, *98*, 15,643–15,665, doi:10.1029/93JA01202.

Challinor, R. A. (1967), The phase velocity and attenuation of audio-frequency electromagnetic waves from simultaneous observations of atmospherics at two spaced stations, *J. Atmos. Terr. Phys.*, *29*, 803–810, doi:10.1016/0021-9169(67)90046-3.

Dmitriev, A.V., and J. K. Chao (2003), Dependence of geosynchronous relativistic electron enhancements on geomagnetic parameters, *J. Geophys. Res.*, *108*(A11), 1388, doi:10.1029/2002JA009664.

Golden, D. I., M. Spasojevic, W. Li, and Y. Nishimura (2012), Statistical modeling of plasmaspheric hiss amplitude using solar wind measurements and geomagnetic indices, *Geophys. Res. Lett.*, *39*, L06103, doi:10.1029/2012GL051185.

Hastie, T., R. Tibshirani, and J. Friedman (2009), *The Elements of Statistical Learning: Data Mining, Inference, and Prediction*, *Springer Ser. in Stat.*, 2nd ed., 745 pp., Springer, New York.

Hocking, R. R. (1976), The analysis and selection of variables in linear regression, *Biometrics*, *32*, 1–49.

Horne, R. B., R. M. Thorne, S. A. Glauert, J. M. Albert, N. P. Meredith, and R. R. Anderson (2005), Time scale for radiation belt electron acceleration by whistler mode chorus waves, *J. Geophys. Res.*, *110*, A03225, doi:10.1029/2004JA010811.

Horne, R. B., S. A. Glauert, N. P. Meredith, D. Boscher, V. Maget, D. Heynderickx, and D. Pitchford (2013), Space weather impacts on satellites and forecasting the Earth's electron radiation belts with SPACECAST, *Space Weather*, *11*, 169–186, doi:10.1002/swe.20023.

Iles, R. H. A., A. N. Fazakerley, A. D. Johnstone, N. P. Meredith, and P. Buhler (2002), The relativistic electron response in the outer radiation belt during magnetic storms, *Ann. Geophys.*, *20*, 957.

Kellerman, A. C., and Y. Y. Shprits (2012), On the influence of solar wind conditions on the outer-electron radiation belt, *J. Geophys. Res.*, *117*, A05217, doi:10.1029/2011JA017253.

Kessel, R. L. (2012), NASA's radiation belt storm probes mission: From concept to reality, in *Dynamics of the Earth's Radiation Belts and Inner Magnetosphere*, *Geophys. Mongr. Ser.*, vol. 199, edited by D. Summers et al., pp. 93–101, AGU, Washington, D. C.

Kozyreva, O. V., V. A. Pilipenko, M. J. Engebretson, and K. Yumoto (2007), A new ULF wave index and its comparison with dynamics of geostationary relativistic electrons, *Planet. Space Sci.*, *55*, 755–769.

Li, L. Y., J. B. Cao, G. C. Zhou, and X. Li (2009), Statistical roles of storms and substorms in changing the entire outer zone relativistic electron population, *J. Geophys. Res.*, *114*, A12214, doi:10.1029/2009JA014333.

Li, W., et al. (2014), Radiation belt electron acceleration by chorus waves during the 17 March 2013 storm, *J. Geophys. Res. Space Physics*, *119*, 4681–4693, doi:10.1002/2014JA019945.

Lyatsky, W., and G. V. Khazanov (2008a), Effect of solar wind density on relativistic electrons at geosynchronous orbit, *Geophys. Res. Lett.*, *35*, L03109, doi:10.1029/2007GL032524.

Lyatsky, W., and G. V. Khazanov (2008b), Effect of geomagnetic disturbances and solar wind density on relativistic electrons at geostationary orbit, *J. Geophys. Res.*, *113*, A08224, doi:10.1029/2008JA013048.

Lyons, L. R., D.-Y. Lee, R. M. Thorne, R. B. Horne, and A. J. Smith (2005), Solar wind-magnetosphere coupling leading to relativistic electron energization during high-speed streams, *J. Geophys. Res.*, *110*, A11202, doi:10.1029/2005JA011254.

Mathie, R. A., and I. R. Mann (2000), A correlation between extended intervals of ULF wave power and storm time geosynchronous relativistic electron flux enhancements, *Geophys. Res. Lett.*, *27*, 3261–3264, doi:10.1029/2000GL003822.

McPherron, R. L., D. N. Baker, and N. U. Crooker (2009), Role of the Russell-McPherron effect in the acceleration of relativistic electrons, *J. Atmos. Sol. Terr. Phys.*, *71*, 1032–1044.

Meredith, N. P., M. Cain, R. B. Horne, R. M. Thorne, D. Summers, and R. R. Anderson (2003), Evidence for chorus-driven electron acceleration to relativistic energies from a survey of geomagnetically disturbed periods, *J. Geophys. Res.*, *108*(A6), 1248, doi:10.1029/2002JA009764.

Miyoshi, Y., and R. Kataoka (2008), Flux enhancement of the outer radiation belt electrons after the arrival of stream interaction regions, *J. Geophys. Res.*, *113*, A03S09, doi:10.1029/2007JA012506.

Miyoshi, Y., R. Kataoka, Y. Kasahara, A. Kumamoto, T. Nagai, and M. F. Thomsen (2013), High-speed solar wind with southward interplanetary magnetic field causes relativistic electron flux enhancement of the outer radiation belt via enhanced condition of whistler waves, *Geophys. Res. Lett.*, *40*, 4520–4525, doi:10.1002/grl.50916.

Neter, J., W. Wasserman, and M. H. Kutner (1985), *Applied Linear Statistical Models*, 1127 pp., Richard D. Irwin, Inc., Homewood, Ill.

O'Brien, T. P., R. L. McPherron, D. Sornette, G. D. Reeves, R. Friedel, and H. J. Singer (2001), Which magnetic storms produce relativistic electrons at geosynchronous orbit?, *J. Geophys. Res.*, *106*, 15,533–15,544, doi:10.1029/2001JA000052.

O'Brien, T. P., K. R. Lorentzen, I. R. Mann, N. P. Meredith, J. B. Blake, J. F. Fennell, M. D. Looper, D. K. Milling, and R. R. Anderson (2003), Energization of relativistic electrons in the presence of ULF power and MeV microbursts: Evidence for dual ULF and VLF acceleration, *J. Geophys. Res.*, *108*(A8), 1329, doi:10.1029/2002JA009784.

Potapov, A. S., B. Tsegmed, and L. V. Ryzhakova (2012), Relationship between the fluxes of relativistic electrons at geosynchronous orbit and the level of ULF activity on the Earth's surface and in the solar wind during the 23rd solar activity cycle, *Cosmic Res.*, *50*(2), 124–140.

Potapov, A. S., B. Tsegmed, and L. V. Ryzhakova (2014), Solar cycle variation of "killer" electrons at geosynchronous orbit and electron flux correlation with the solar wind parameters and ULF waves intensity, *Acta Astronaut.*, *93*, 55–63.

Reeves, G. D., K. L. McAdams, and R. H. W. Friedel (2003), Acceleration and loss of relativistic electrons during geomagnetic storms, *Geophys. Res. Lett.*, *30*(10), 1529, doi:10.1029/2002GL016513.

Reeves, G. D., S. K. Morley, R. H. W. Friedel, M. G. Henderson, T. E. Cayton, G. Cunningham, J. B. Blake, R. A. Christensen, and D. Thomsen (2011), On the relationship between relativistic electron flux and solar wind velocity: Paulikas and Blake revisited, *J. Geophys. Res.*, *116*, A02213, doi:10.1029/2010JA015735.

Rodger, C. J., B. R. Carson, S. A. Cummer, R. J. Gamble, M. A. Clilverd, J. C. Green, J.-A. Sauvaud, M. Parrot, and J.-J. Berthelier (2010), Contrasting the efficiency of radiation belt losses caused by ducted and nonducted whistler mode waves from ground-based transmitters, *J. Geophys. Res.*, *115*, A12208, doi:10.1029/2010JA015880.

Romanova, N., and V. Pilipenko (2008), ULF wave indices to characterize the solar wind: Magnetosphere interaction and relativistic electron dynamics, *Acta Geophys.*, *57*(1), 158–170, doi:10.2478/s11600-008-0064-4.

Rostoker, G., S. Skone, and D. N. Baker (1998), On the origin of relativistic electrons in the magnetosphere associated with some geomagnetic storms, *Geophys. Res. Lett.*, *25*, 3701–3704, doi:10.1029/98GL02801.

Russell, C. T., and R. L. McPherron (1973), Semiannual variation of geomagnetic activity, *J. Geophys. Res.*, *78*, 92–108, doi:10.1029/JA078i001p00092.

Simms, L. E., V. A. Pilipenko, and M. J. Engebretson (2010), Determining the key drivers of magnetospheric Pc5 wave power, *J. Geophys. Res.*, *115*, A10241, doi:10.1029/2009JA015025.

Simms, L. E., V. A. Pilipenko, M. J. Engebretson, G. D. Reeves, A. J. Smith, and M. Clilverd (2014), Prediction of relativistic electron flux at geostationary orbit following storms: Multiple regression analysis, *J. Geophys. Res. Space Physics*, *119*, 7297–7318, doi:10.1002/2014JA019955.

Smith, A. J. (1995), VELOX: A new VLF/ELF receiver in Antarctica for the Global Geospace Science mission, *J. Atmos. Terr. Phys.*, *57*(5), 507–524.

Smith, A. J., N. P. Meredith, and T. P. O'Brien (2004), Differences in ground-observed chorus in geomagnetic storms with and without enhanced relativistic electron fluxes, *J. Geophys. Res.*, *109*, A11204, doi:10.1029/2004JA010491.

Smith, A. J., R. B. Horne, and N. P. Meredith (2010), The statistics of natural ELF/VLF waves derived from a long continuous set of ground-based observations at high latitude, *J. Atmos. Terr. Phys.*, *72*, 463–475.

Sokal, R. R., and F. J. Rohlf (1995), *Biometry: The Principles and Practice of Statistics in Biological Research*, 3rd ed., 859 pp., W. H. Freeman, New York.

Su, Z., et al. (2014), Intense duskside lower band chorus waves observed by Van Allen Probes: Generation and potential acceleration effect on radiation belt electrons, *J. Geophys. Res. Space Physics*, *119*, 4266–4273, doi:10.1002/2014JA019919.

Thorne, R. M., et al. (2013), Rapid local acceleration of relativistic radiation-belt electrons by magnetospheric chorus, *Nature*, *504*, 411, doi:10.1038/nature12889.

Tu, W., G. S. Cunningham, Y. Chen, S. K. Morley, G. D. Reeves, J. B. Blake, D. N. Baker, and H. Spence (2014), Event-specific chorus wave and electron seed population models in DREAM3D using the Van Allen Probes, *Geophys. Res. Lett.*, *41*, 1359–1366, doi:10.1002/2013GL058819.

Turner, D. L., et al. (2014), Competing source and loss mechanisms due to wave-particle interactions in Earth's outer radiation belt during the 30 September to 3 October 2012 geomagnetic storm, *J. Geophys. Res. Space Physics*, *119*, 1960–1979, doi:10.1002/2014JA019770.

Ukhorskiy, A. Y., M. I. Sitnov, A. S. Sharma, B. J. Anderson, S. Ohtani, and A. T. Y. Lui (2004), Data-derived forecasting model for relativistic electron intensity at geosynchronous orbit, *Geophys. Res. Lett.*, *31*, L09806, doi:10.1029/2004GL019616.

Walker, A. D. M. (1971), The propagation of very low-frequency radio waves in ducts in the magnetosphere, *Proc. R. Soc. London, Ser. A*, *321*(1544), 69–93.

Weigel, R. S., A. J. Klimas, and D. Vassiliadis (2003), Precursor analysis and prediction of large-amplitude relativistic electron fluxes, *Space Weather*, *1*(3), 1014, doi:10.1029/2003SW000023.

Xiao, F., et al. (2014), Chorus acceleration of radiation belt relativistic electrons during March 2013 geomagnetic storm, *J. Geophys. Res. Space Physics*, *119*, 3325–3332, doi:10.1002/2014JA019822.